

# Efficient MoM simulation of 3D metallic antenna connected to finite ground plane

Jean Cavillot, Christophe Craeye

*ICTEAM*

*Université catholique de Louvain*

Louvain-la-Neuve, Belgium

jean.cavillot@uclouvain.be,

christophe.craeye@uclouvain.be

Eloy de Lera Acedo, Nima Razavi-Ghods

*Department of Physics*

*University of Cambridge*

Cambridge, UK

eloy@mrao.cam.ac.uk,

nima@mrao.cam.ac.uk

**Abstract**—An efficient method is presented to simulate a 3D antenna connected to a finite ground plane itself lying on a layered medium. The spectral interactions between equivalent currents of the antenna and the finite ground plane are accelerated thanks to an asymptotic extraction of the integrated spectrum. The term accounting for the asymptotic part is obtained in free-space. Besides, efficient techniques for finite ground planes of canonical shapes cannot be considered in this case because the connection between the ground plane and the antenna is established with a fine mesh region which breaks the symmetries of the finite ground plane equivalent currents. Here a method to remedy this issue and which efficiently simulates defected rectangular ground planes is presented. The method is based on Toeplitz matrices and the defect is taken into account by exploiting a memory-efficient direct method.

**Index Terms**—Method of Moments, Finite ground plane, Inhomogeneous plane waves, Toeplitz

## I. INTRODUCTION

Many applications including radio astronomy [1] and synthetic aperture radars (SAR) [2] use 3D metallic antennas on top of finite platforms. The finite aspect of the platform has an impact on the antenna input impedance and radiation pattern. These effects are usually taken into account using the method of images which assumes an infinite ground plane. In some cases, this assumption is too restrictive and the antenna parameters are significantly different when considering the finite aspect of the ground plane. For example, this can have a serious impact if the antennas are used for pattern-nulling. The performance will deteriorate if the pattern zeroes obtained with the infinite ground plane assumption are in practice shifted or degraded due to the finite platform aspect. This issue is of great importance in applications like radio astronomy where pattern-nulling is used to cancel interferences from unwanted sources such as the sun in order to achieve high sensitivity. Accurate pattern nulling [3] is also of great importance in telecommunication systems to cancel interference with undesired sources while receiving a signal from a given direction. A good knowledge of the pattern which includes the finite ground plane can prevent the degradation of the signal-to-noise ratio.

This work was supported by the FRIA (Fonds pour la formation à la Recherche dans l'Industrie et l'Agriculture) grant from the Belgium FNRS (Fonds National de la Recherche Scientifique).

Finite ground planes are electrically large objects, which means that their inclusion in the simulation model alters the performance in terms of memory storage and simulation time. That is why solvers based on the integral equations (IEs) such as the classical Method of Moments (MoM), known for their accuracy, are inconvenient in those problems. Previously, asymptotic methods including the uniform theory of diffraction (UTD) were used to study the impact of the ground plane [4], [5]. Other techniques separate the problem into two distinct domains: one domain corresponding to the antenna and its direct surrounding where the MoM is used and one domain corresponding to the platform where the physical optics (PO) is applied [6]. The results obtained with this technique can be improved by iterating between those two regions [7]. Hybridized techniques based on multilevel fast multipoles were also used to simulate arrays on large and complex platforms [8].

In radio astronomy, some experiments are conducted with a single antenna lying on a finite ground plane, itself lying on soil [9]–[11]. The soil is generally modeled as a layered medium, which means that the spectral formulation of the MoM is more convenient in this situation. In [12], [13] a spectral method based on inhomogeneous plane waves is developed to compute the MoM interactions between the antenna and the finite ground plane. In this formulation, the soil is taken into account through a wavenumber-dependent reflection coefficient. While this method shows great efficiency when there is some distance between the antenna equivalent currents and the ground plane, its performance degrades when the antenna is directly connected to the ground plane. In that case, the plane wave spectrum that needs to be integrated to compute the interactions between equivalent currents close to the ground plane and the ground plane itself is slowly converging and a great number of integration points is needed. In this paper, we consider that the antenna is connected to the ground plane through strictly vertical conductors. This allows one to apply a Kummer extraction, which consists of directly extracting an asymptotic part of the spectrum of interaction and accounting for it in free-space [14].

Once the interactions between the antenna and the ground plane are calculated, the MoM linear system of equations can

be solved. Efficient methods have been used to solve the MoM for canonical shapes of the finite ground plane [13], [15]. However, when the antenna is directly connected to the ground plane, a fine mesh region is established at the connection points and the translational or rotational symmetries of the ground plane equivalent currents are broken. Here we remedy this problem by creating an artificial defect in a regular ground plane where the fine mesh region can be placed. This defect is taken into account using direct methods afterwards.

## II. METHOD OF MOMENTS

### A. Antenna connected to ground plane

Let us consider a 3D metallic antenna connected to a finite ground plane [9], [10] as depicted in Figs. 1, 2. We consider a frequency of 60 MHz. The antenna is divided into four regions: the top of the antenna (green region), the bottom of the antenna (red region), the fine mesh region connecting the antenna to the ground plane (black region) and the ground plane (blue region). The red region corresponds to all equivalent currents located below the plane  $z = \lambda_0/20$  where  $\lambda_0$  is the free space wavelength. The ground plane is lying on top of a semi-infinite or multilayered soil. The MoM system of linear equations reads:

$$\begin{bmatrix} \mathbf{Z}_{bb} & \mathbf{Z}_{bk} & \mathbf{Z}_{br} & \mathbf{Z}_{bg} \\ \mathbf{Z}_{kb} & \mathbf{Z}_{kk} & \mathbf{Z}_{kr} & \mathbf{Z}_{kg} \\ \mathbf{Z}_{rb} & \mathbf{Z}_{rk} & \mathbf{Z}_{rr} & \mathbf{Z}_{rg} \\ \mathbf{Z}_{gb} & \mathbf{Z}_{gk} & \mathbf{Z}_{gr} & \mathbf{Z}_{gg} \end{bmatrix} \mathbf{i} = \mathbf{v}, \quad (1)$$

where  $\mathbf{Z}_{mn}$  is a the MoM matrix of interactions between regions  $\mathbf{m}$  and  $\mathbf{n}$ . The subscripts  $\mathbf{b}, \mathbf{k}, \mathbf{r}, \mathbf{g}$  correspond to the blue, black, red and green regions, respectively.  $\mathbf{i}$  contains the current coefficient and  $\mathbf{v}$  is the excitation vector.

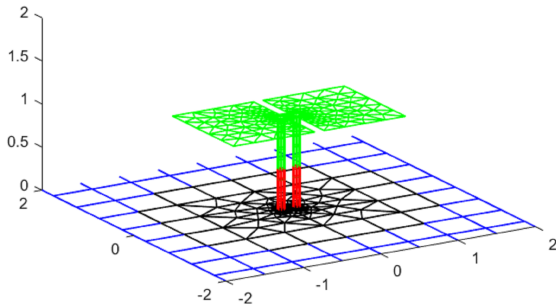


Fig. 1. 3D metallic antenna lying on finite ground plane.

### B. Interactions using inhomogeneous plane waves

The MoM interactions between the green part and the blue or the black parts can be computed using inhomogeneous plane waves. Using the mathematical definitions of [12], [16], [17]

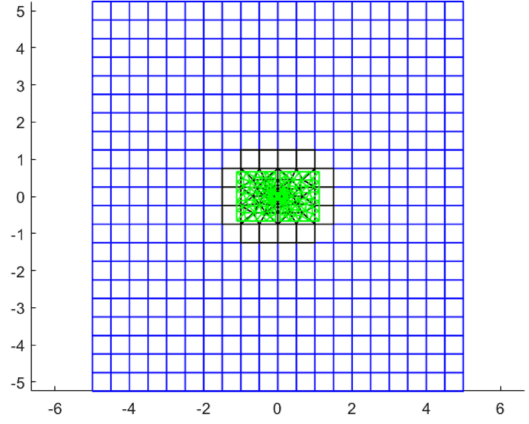


Fig. 2. 3D metallic antenna lying on finite ground plane: top view.

the interaction between the green part of the antenna and the blue region read:

$$\mathbf{Z}_{gb} = \frac{-j k_0 \eta_0}{(2\pi)^2} \iint \left[ F_{g,TE} F_{b,TE}^{**} (1 + \Gamma_{TE}) + F_{g,TM} F_{b,TM}^{**} (1 - \Gamma_{TM}) \right] \frac{1}{2jk_z} dk_x dk_y \quad (2)$$

where  $k_0$  is the free space wavenumber,  $\eta_0$  is the free space impedance,  $\Gamma_p$  is the reflection coefficient for polarization  $p$  (TE or TM) due to the presence of the soil [18].  $F_{g,p}$  and  $F_{b,p}^{**}$  are defined as the radiation patterns with polarization  $p$  of the green and blue domains respectively. The radiation patterns  $F_{R,p}$  and  $F_{R,p}^{**}$  of a given region  $R$  are defined as follows:

$$F_{R,p}(k_x, k_y) = \iiint_{V'} \hat{\mathbf{e}}_p^d \cdot \vec{J}_R(\vec{r}') e^{j(k_x x' + k_y y' - k_z z')} dV', \quad (3)$$

$$F_{R,p}^{**}(k_x, k_y) = \iiint_{V'} \hat{\mathbf{e}}_p^u \cdot \vec{J}_R(\vec{r}') e^{-j(k_x x' + k_y y' - k_z z')} dV', \quad (4)$$

where  $\vec{J}_R(\vec{r}')$  is the current density of the region  $R$ ,  $\hat{\mathbf{e}}_p$  is the polarization vector of polarization  $\mathbf{p}$  and the superscripts  $\mathbf{u}, \mathbf{d}$  indicate upwards or downwards propagating waves, respectively [16].

### C. Kummer extraction combined with inhomogeneous plane waves

When considering the MoM interactions between the red part of Fig. 1 and the ground plane, the inhomogeneous plane waves method loses its efficiency. Indeed the equivalent currents of the antenna are very close to the ground plane which means that the inhomogeneous plane waves spectrum to integrate is slowly converging and requires more integration points. In this paper, we use a Kummer extraction that allows one to account for the asymptotic part of the spectrum through a weighted free-space term [14]. After extraction of the asymptotic part, the filtered spectrum can be integrated with inhomogeneous plane waves.

Let us consider the interaction between the vertical equivalent currents of the red region and the ground plane, the MoM matrix of interaction can be obtained as follows:

$$\mathbf{Z}_{\text{rb}} = \frac{-j k_0 \eta_0}{(2\pi)^2} \iint \left[ F_{r, TM} F_{b, TM}^{**} (1 - \Gamma_{TM}) \right] \frac{1}{2jk_z} dk_x dk_y. \quad (5)$$

This equation only contains TM polarization because the electric field radiated by vertical equivalent currents only produces a TM component. Thanks to this property, equation (5) can be decomposed into two terms. In the first term, the asymptotic part of the inhomogeneous plane waves spectrum is removed:

$$\mathbf{Z}_{\text{rb}}^{\text{filt}} = \frac{-j k_0 \eta_0}{(2\pi)^2} \iint \left[ F_{r, TM} F_{b, TM}^{**} ((1 - \Gamma_{TM}) - (1 - \Gamma_{TM}^{\text{as}})) \right] \frac{1}{2jk_z} dk_x dk_y, \quad (6)$$

where the superscript **filt** indicates that the spectrum is filtered and where  $\Gamma_{TM}^{\text{as}}$  corresponds to the asymptotic part of the reflection coefficient and is not wavenumber-dependent. The second term compensates for the removal of the asymptotic part and corresponds to the free space interaction matrix multiplied by a constant:

$$\mathbf{Z}_{\text{rb}}^{\text{as}} = (1 - \Gamma_{TM}^{\text{as}}) \mathbf{Z}_{\text{rb}}^{\text{fs}}, \quad (7)$$

where the superscript **fs** indicates that the interactions are computed in free-space. Finally, these results are added up to obtain:

$$\mathbf{Z}_{\text{rb}} = \mathbf{Z}_{\text{rb}}^{\text{filt}} + \mathbf{Z}_{\text{rb}}^{\text{as}}. \quad (8)$$

The filtering effect is illustrated for the Green's function in Fig. 3. For this result, we consider a semi-infinite soil of relative permittivity  $\epsilon_r = 4.8$ . In this case,  $\Gamma_{TM}^{\text{as}} = (\epsilon_r - 1)/(\epsilon_r + 1)$ . The blue curve is the Green's function, the red curve approximates the asymptotic part of the Green's function and the yellow curve is the difference between the first two curves.

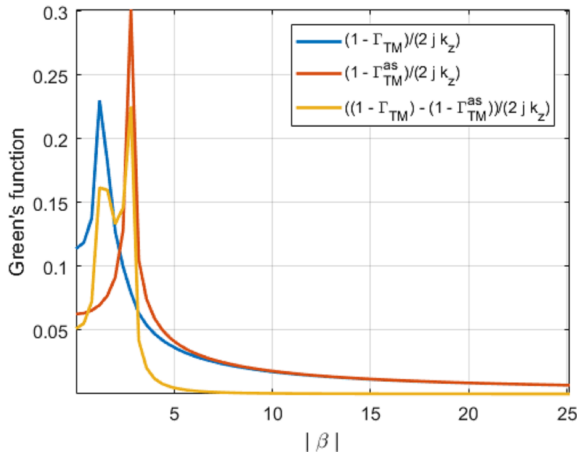


Fig. 3. Spectral Green's function: asymptotic extraction.

#### D. Defected rectangular ground plane

Let us first consider a perfect rectangular ground plane. If it is meshed with rooftop basis functions and represented with repeating smaller rectangular domains [15], the ground plane MoM matrix of interactions is Toeplitz-block Toeplitz:

$$\mathbf{T} = \begin{bmatrix} \mathbf{T}_{11} & \mathbf{T}_{12} & \cdots & \cdots & \mathbf{T}_{1N} \\ \mathbf{T}_{21} & \mathbf{T}_{11} & \mathbf{T}_{12} & \cdots & \mathbf{T}_{2N} \\ \vdots & \mathbf{T}_{21} & \mathbf{T}_{11} & \ddots & \vdots \\ \vdots & \ddots & \ddots & \ddots & \mathbf{T}_{12} \\ \mathbf{T}_{N1} & \mathbf{T}_{N2} & \cdots & \mathbf{T}_{21} & \mathbf{T}_{11} \end{bmatrix} \quad (9)$$

with  $N$  the number of repeated rectangular domains and  $\mathbf{T}_{ij}$  denoting the interaction between domain  $i$  and domain  $j$ . This property enables the low memory storage of the inverse of  $\mathbf{T}$ , which can be written as a sum of products of block-circulant matrices [15], [19]:

$$\mathbf{T}^{-1} = \frac{1}{2} (\mathbf{M}_1 \mathbf{M}_2 - \mathbf{M}_3 \mathbf{M}_4) \quad (10)$$

where  $\mathbf{M}_2, \mathbf{M}_4$  are block-circulant matrices and  $\mathbf{M}_1, \mathbf{M}_3$  are block skew-circulant matrices. Those matrices can be obtained by solving the systems of linear equations involving the matrix  $\mathbf{T}$  in equations (15)-(18) of [19]. The block-circulant structure of the matrices  $\mathbf{M}_1, \mathbf{M}_2, \mathbf{M}_3, \mathbf{M}_4$  enables the use of the FFT to compute any matrix-vector product with  $\mathbf{T}^{-1}$ . From here, let us suppose that one needs to remove some of the ground plane basis functions to include the black region as shown in Fig. 1. This creates a defect in the finite ground plane and the MoM matrix of interaction of the blue part is no longer Toeplitz-block Toeplitz. This section shows how to efficiently compute the inverse of the MoM matrix associated with the defected rectangular ground plane with low memory storage. In order to take into account the defected region, zeroes are included in the rows of  $\mathbf{T}$  having indices which correspond to the defected region. The new matrix, obtained after the zeroes inclusion in  $\mathbf{T}$ , can be written:

$$\mathbf{E} = (\mathbb{I} - \mathbb{I}_s) \mathbf{T} + \mathbb{I}_s = (\mathbb{I} - \mathbb{I}_s + \mathbb{I}_s \mathbf{T}^{-1}) \mathbf{T} = \mathbf{W} \mathbf{T} \quad (11)$$

where  $\mathbb{I}$  is the identity matrix and  $\mathbb{I}_s$  is a diagonal matrix with ones on the entries corresponding to the defect. From there, the inverse of  $\mathbf{E}$  can be written as follows:

$$\mathbf{E}^{-1} = \mathbf{T}^{-1} (\mathbb{I} - \mathbb{I}_s + \mathbb{I}_s \mathbf{T}^{-1})^{-1} = \mathbf{T}^{-1} \mathbf{W}^{-1}. \quad (12)$$

A compact representation of  $\mathbf{W}^{-1}$  can be found. This representation is composed of the matrix  $\mathbf{T}^{-1}$ , and an additional matrix corresponding to the size of the defect. While this matrix is not easily obtained in terms of computational complexity, this formulation is certainly memory-efficient. Finally, the MoM system of linear equations in (1) can be solved using the Schur's complement [15]. To that end, we first rewrite it as follows:

$$\begin{bmatrix} \mathbf{E} & \mathbf{B} \\ \mathbf{C} & \mathbf{D} \end{bmatrix} \begin{bmatrix} \mathbf{i}_e \\ \mathbf{i}_d \end{bmatrix} = \begin{bmatrix} \mathbf{v}_e \\ \mathbf{v}_d \end{bmatrix}, \quad (13)$$

where the matrix  $\mathbf{E}$  accounts for the defected ground plane and where the matrices  $\mathbf{B}, \mathbf{C}, \mathbf{D}$  account for the antenna and

the black domain. The subscript  $\mathbf{e}$  indicates the defected ground plane and the subscript  $\mathbf{d}$  represents the red, green and black regions (see Fig. 1). Using the Schur's complement, the solution of the linear system of equations can be obtained as follows:

$$\begin{aligned} (-\mathbf{C} \mathbf{T}^{-1} \mathbf{W}^{-1} \mathbf{B} + \mathbf{D}) \mathbf{i}_{\mathbf{d}} &= (\mathbf{v}_{\mathbf{d}} - \mathbf{C} \mathbf{T}^{-1} \mathbf{W}^{-1} \mathbf{v}_{\mathbf{e}}) \\ \mathbf{i}_{\mathbf{e}} &= \mathbf{T}^{-1} \mathbf{W}^{-1} (\mathbf{v}_{\mathbf{t}} - \mathbf{B} \mathbf{i}_{\mathbf{d}}). \end{aligned} \quad (14)$$

where it is assumed that a matrix of same size as  $\mathbf{D}$  is invertible, which is generally the case for classical antennas. The advantage of this method lies in the compact form of the defected ground plane MoM matrix and its fast multiplication with the use of FFTs.

### E. Radiation pattern

Using the methods described above, the radiation pattern of the antenna on a finite ground plane above a semi-infinite soil is calculated. Fig. 4 compares the radiation pattern obtained with the infinite ground plane assumption with the ones obtained with a soil of relative permittivity  $\epsilon_r = 1$  and  $\epsilon_r = 5 - 6j$ . A rectangular ground plane of size  $20 \text{ m} \times 20 \text{ m}$  is selected for the two latter cases. Although the ground plane is relatively large ( $4\lambda_0 \times 4\lambda_0$ ), a significant difference between those three patterns is observed.

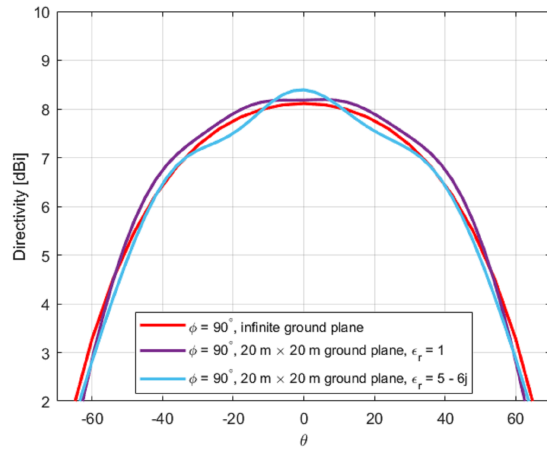


Fig. 4. Comparison of the radiation pattern obtained with the infinite ground plane case, with a  $20 \text{ m} \times 20 \text{ m}$  finite ground plane in free space and above a lossy soil of relative permittivity  $\epsilon_r$ .

## III. CONCLUSION

This paper presents an efficient method to deal with the close range spectral MoM interactions between a 3D antenna and a finite ground plane lying on a layered medium. This method is based on an asymptotic extraction of the integrated spectrum which allows the use of fewer integration points while the asymptotic term is computed in free space. Besides, a technique is presented to benefit from the symmetries of the rectangular ground plane even if that plane is locally defected. It makes use of an interesting property of the

inverse of Toeplitz matrices. The additional memory storage, besides the one needed for the rectangular ground plane (linear complexity), corresponds to a matrix of the size of the defect.

## REFERENCES

- [1] E. de Lera Acedo, N. Razavi-Ghods, N. Troop, N. Drought, and, A. J. Faulkner, "SKALA, a log-periodic array antenna for the SKA-low instrument: design, simulations, tests and system considerations," *Exp. Astron.*, vol. 39, no. 3, pp. 567-594, Jul. 2015.
- [2] T. Paireon, S. Karki, S. Monni and C. Craeye, "Efficient analysis of arrays of compact metallic elements devoted to satellite SAR," *Eur. Conf. on Antennas and Propag. (EuCAP)*, pp. 1-5, 2019.
- [3] H. Bui-Van, V. Hamaide, C. Craeye, F. Glineur and E. de Lera Acedo, "Direct Deterministic Nulling Techniques for Large Random Arrays Including Mutual Coupling," *IEEE Trans. Antennas Propag.*, vol. 66, no. 11, pp. 5869-5878, Nov. 2018.
- [4] N. A. Aboserwal, C. A. Balanis, and C. R. Birtcher, "Impact of finite ground plane edge diffraction on radiation patterns of aperture antennas," *Progress In Electromagnetics Research B*, no. 55, pp. 1-21, 2013.
- [5] H. M. Ibrahim and D. T. Stephenson, "Radiation patterns of a  $\lambda/4$  monopole mounted on thick finite square or circular ground plane," *Int. J. Electronics*, vol. 64, no. 3, pp. 345-358, Jul. 1988.
- [6] T. Paireon, J. Cavillot, S. Karki and C. Craeye, "Effect of finite ground plane on irregular arrays with metallic elements," *Proc. Int. Conf. Electromag. in Ad. App. (ICEAA)*, pp. 1122-1125, Sep. 2019.
- [7] Z. Liu and C. Wang, "An efficient iterative MoM-PO hybrid method for analysis of an onboard wire antenna array on a large-scale platform above an infinite ground," *IEEE Antennas Propag. Mag.*, vol. 55, no. 6, pp. 69-78, Dec. 2013.
- [8] X. Zhao, Z. Lin, Y. Zhang, S. Ting and T. K. Sarkar, "Parallel hybrid method of HOMoM-MLFMA for analysis of large antenna arrays on an electrically large platform," *IEEE Trans. Antennas Propag.*, vol. 64, no. 12, pp. 5501-5506, Dec. 2016.
- [9] A. E. E. Rogers and J. D. Bowman, "Absolute calibration of a wideband antenna and spectrometer for accurate sky noise temperature measurements," *Radio Science*, vol. 47, Jul. 2012.
- [10] J. D. Bowman, A. E. E. Rogers, R. A. Monsalve, T. J. Mozdzen and N. Mahesh, "An absorption profile centred at 78 megahertz in the sky-averaged spectrum," *Nature*, vol. 555, no 7694, p. 67-70, Mar. 2018.
- [11] E. de Lera Acedo, "REACH: Radio Experiment for the Analysis of Cosmic Hydrogen," *Proc. Int. Conf. Electromag. in Ad. App. (ICEAA)*, pp. 0742-0745, Sep. 2019.
- [12] J. Cavillot, H. Bui-Van, C. Craeye, H. Pienaar, and E. de Lera Acedo, "Efficient analysis of a 3D antenna installed on a finite ground plane," *Eur. Conf. on Antennas and Propag. (EuCAP)*, London, 2018.
- [13] J. Cavillot, D. Tihon, F. Mesa, E. De Lera Acedo and C. Craeye, "Efficient Simulation of Large Irregular Arrays on a Finite Ground Plane," *IEEE Trans. Antennas Propag.*, vol. 68, no. 4, pp. 2753-2764, Apr. 2020.
- [14] Y. L. Chow, J. J. Yang, D. G. Fang and G. E. Howard, "A closed-form spatial Green's function for the thick microstrip substrate," *IEEE Trans. on Microw. Theory and Tech.*, vol. 39, no. 3, pp. 588-592, Mar. 1991.
- [15] J. Cavillot, D. Tihon, C. Craeye, E. de Lera Acedo and N. Razavi-Ghods, "Fast simulation technique for antenna installed on a finite ground plane," *Proc. Int. Conf. Electromag. in Ad. App. (ICEAA)*, pp. 0742-0745, Sep. 2019.
- [16] K. Alkhalifeh, G. Hislop, N. A. Ozdemir, and C. Craeye, "Efficient MoM simulation of 3-D antennas in the vicinity of the ground," *IEEE Trans. Antennas Propag.*, vol. 64, pp. 5335 - 5344, Dec. 2016.
- [17] S. Karki and C. Craeye, "Macro Basis Function interactions accelerated with the inhomogeneous plane waves," *Proc. Int. Conf. Electromag. in Ad. App. (ICEAA)*, Sept 2015.
- [18] K.A. Michalski and J.R. Mosig, "Multilayered media Green's functions in integral equation formulations," *IEEE Trans. Antennas Propag.*, vol. 45, no. 3, pp. 508-519, Mar. 1997.
- [19] X. Lv and T. Huang, "The inverses of block Toeplitz matrices," *Journal of Mathematics*, vol. 13, no. ID 207176, 2013.